Uncertain dynamical systems in the medium-frequency range

Christian Soize

UNCERTAIN DYNAMICAL SYSTEMS IN THE MEDIUM-FREQUENCY RANGE

by

C. Soize

Laboratoire de Mécanique, Université de Marne-la-Vallée, 5 Bd Descartes,
77454 Marne-la-Vallée Cedex, France - E-mail: soize@univ-mlv.fr

Key Words: Medium-frequency dynamics, Random uncertainties

Abstract: This paper presents a novel probabilistic model of random uncertainties for dynamical system in the medium-frequency (MF) range. This approach combines a nonparametric probabilistic model of random uncertainties for the reduced matrix models in structural dynamics with a reduced matrix model adapted to the MF range. The theory is presented, the random energy matrix relating to a given MF band, its random trace and its random eigenvalues are studied. A numerical example is presented allowing convergence properties and stability of random responses with respect to the bandwith to be analyzed.

INTRODUCTION

In linear structural dynamics, it is known that the higher the eigenfrequency of a structural mode, the lower its accuracy because the uncertainties in the model increase. The effects of uncertainties (geometrical parameters; boundary conditions; mass density; mechanical parameters of constitutive equations; structural complexity; interface and junction modeling; etc.) increase with the frequency and it should be kept in mind that the mechanical model and the ¿nite element model of a complex structure tend to be less reliable in predicting the higher structural modes. This paper is devoted to linear structural dynamics in the medium-frequency range. A detailed description and a de¿nition of the medium-frequency range are given in the book (Ohayon & Soize 1998). Consequently, for the medium-frequency dynamics, random uncertainties in the mechanical model have to be taken into account in order to improve the

ef¿ciency and the robustness of the medium-frequency ¿nite element models. An important aspect of the medium-frequency (MF) domain is the construction of an ef¿cient reduced matrix model of the continuous dynamical system. For the low-frequency (LF) dynamic analysis, it is known that the reduced matrix models constitute a very ef¿cient tool for constructing the dynamical response (see for instance Clough & Penzien 1975; Argyris & Mlejnek 1991) . These techniques correspond to a Ritz-Galerkin reduction of the structural-dynamics model using the structural modes corresponding to the lowest eigenfrequencies of the associated conservative dynamical system. Unfortunately, this modal method which is very ef¿cient in the LF domain, can be dif¿cult to use in the MF domain for general three-dimensional dynamical systems (see Ohayon & Soize 1998). In this context, for general dissipative dynamical systems, a reduced matrix model adapted to the MF range, was proposed by (Soize 1998). Such a reduced matrix model is based on the use of the dominant eigensubspace of the mechanical energy operator (or the energy matrix for the discretized system) relating to the MF band.

Recently, a parametric approach of random uncertainties in MF dynamics has been proposed by (Ghanem & Sarkar 2003) using reduced matrix models combined with the stochastic ¿nite element method (Ghanem & Spanos 1991; Ghanem 1999), consisting in a stochastic reduction of the random uncertainties utilizing the Karhunen-Loeve expansion (Guikhman & Skorokhod 1979) and solving the reduced random matrix equation with the polynomial chaos expansion (Ghanem & Spanos 1991; Cameron & Martin 1947).

In this paper, we propose an alternative approach concerning random uncertainties modeling in MF dynamics, which results from the use of the nonparametric probabilistic model of random uncertainties for the reduced matrix models in structural dynamics (Soize 2000 & 2001) and combined with the reduced matrix model method in the MF range developed in (Soize 1998). In addition, the random eigenvalues and the random trace of the random energy operator of the stochastic system, relating to the medium-frequency band, are studied. This random energy matrix is independent of any given load.

In a ¿rst part, the proposed theory for the medium-frequency dynamics of a stochastic system subjected to a given deterministic load is presented. A convergence analysis criterium and the con¿dence region of the random accelerations of the stochastic system are introduced. The second part deals with the random energy matrix (the matrix of the random energy operator of

the discretized stochastic dynamical system). This random energy matrix is a random matrix with values in the set of all the positive symmetric square real matrices and is an intrinsic quantity which is independent of any given load. Consequently, the random eigenvalues of this random energy matrix are positive-valued random variables and the random trace of this random energy matrix, which is equal to the sum of its random eigenvalues, is an important scalar quantity characterizing the stochastic dynamical system. Therefore, the probability distribution of this random trace is studied. In a last part, a numerical example is presented: (1) The random MF response of the stochastic system subjected to a given deterministic load is constructed and a convergence analysis is performed. A sensitivity analysis of this random MF response is carried out with respect to the dispersion parameters of the nonparametric model of random uncertainties of the dynamical system. (2) Then, the random eigenvalues and the random trace of the random energy matrix are analyzed. The probability density function of the random trace is estimated. A sensitivity analysis of this random trace is carried out with respect to the dispersion parameters of the nonparametric model. (3) Finally, since the medium-frequency analysis is performed medium-frequency band by medium-frequency band, the stability of the random response with respect to the bandwith of the medium-frequency band is presented.

RANDOM MEDIUM-FREQUENCY RESPONSE OF A STOCHASTIC SYSTEM SUBJECTED TO A PRESCRIBED EXTERNAL DETERMINISTIC LOAD

Mean model of the dynamical system and its mean ¿nite element model

In the medium-frequency band $B = [\omega_{\min}\,,\,\omega_{\max}]$ with $\omega_{\min} \gg \omega_{\max} - \omega_{\min} > 0$, the mean ¿nite element model of linear vibrations of a viscoelastic bounded structure (¿xed or free) around a position of static equilibrium taken as reference con¿guration without prestresses is written as

$$\left(-\omega^2\,[\,\underline{\mathbb{M}}\,] + i\omega\,[\underline{\mathbb{D}}(\omega)] + [\underline{\mathbb{K}}(\omega)]\,\right)\,\underline{\mathbf{y}}(\omega) = \underline{\mathbf{f}}(\omega) \quad , \quad \omega \in B \quad , \tag{1}$$

in which $\underline{\mathbf{y}}(\omega) = (\underline{y}_1(\omega), \ldots, \underline{y}_m(\omega))$ is the $\mathbb{C}^m$-vector of the m DOFs (displacements and/or rotations) and $\underline{\mathbf{f}}(\omega) = (\underline{f}_1(\omega), \ldots, \underline{f}_m(\omega))$ is the $\mathbb{C}^m$-vector of the m inputs (forces and/or moments). The mean mass matrix $[\,\underline{\mathbb{M}}\,]$ is a positive-de¿nite symmetric $(m \times m)$ real matrix. The mean damping and stiffness matrices $[\underline{\mathbb{D}}(\omega)]$ and $[\underline{\mathbb{K}}(\omega)]$ are symmetric $(m \times m)$ real matrices, depend on ω (viscoelastic structure), are such that $[\underline{\mathbb{D}}(-\omega)] = [\underline{\mathbb{D}}(\omega)]$ and $[\underline{\mathbb{K}}(-\omega)] = [\underline{\mathbb{K}}(\omega)]$, and

are either positive de¿nite (¿xed structure) or positive semide¿nite (free structure). In the case of a free structure, for all ω in B, (1) matrices $[\underline{\mathbb{D}}(\omega)]$ and $[\underline{\mathbb{K}}(\omega)]$ have the same null space having a dimension m_{rig} such that $0 < m_{\text{rig}} \leq 6$ and spanned by the rigid body modes $\{\mathbf{y}_1, \ldots, \mathbf{y}_{m_{\text{rig}}}\}$ and (2) given deterministic load vector $\underline{\mathbf{f}}(\omega)$ is in equilibrium, i.e. is such that $<\underline{\mathbf{f}}(\omega)\,,\mathbf{y}_\alpha>=0$ for all α in $\{1,\ldots,m_{\text{rig}}\}$, in which, for all $\mathbf{u}$ and $\mathbf{v}$ in $\mathbb{C}^m$, $<\mathbf{u}\,,\mathbf{v}>=u_1\,v_1+\ldots+u_m\,v_m$. For all ω in B, Eq. (1) has a unique solution $\underline{\mathbf{y}}(\omega) = [\underline{\mathbb{T}}(\omega)]\,\underline{\mathbf{f}}(\omega)$ in which $[\underline{\mathbb{T}}(\omega)]$ is the matrix-valued FRF (frequency response function) de¿ned by $[\underline{\mathbb{T}}(\omega)] = [\underline{\mathbb{A}}(\omega)]^{-1}$ where $[\underline{\mathbb{A}}(\omega)]$ is the dynamic stiffness matrix such that $[\underline{\mathbb{A}}(\omega)] = -\omega^2\,[\,\underline{\mathbb{M}}\,]+i\omega\,[\underline{\mathbb{D}}(\omega)]+[\underline{\mathbb{K}}(\omega)]$. For a ¿xed or a free structure, and for every ω ¿xed in B, the sparse complex matrix $[\underline{\mathbb{A}}(\omega)]$ is invertible.

Mean reduced matrix model adapted to an MF band

In MF band B, the energy matrix $[\underline{\mathbb{E}}_B]$ (twice the kinetic energy) of the mean FEM is the positive-de¿nite symmetric $(m \times m)$ real matrix which is written (see Soize 1998) as

$$[\underline{\mathbb{E}}_B] = \frac{1}{\pi}\int_B \omega^2\,\Re e\,\{[\underline{\mathbb{T}}(\omega)]^*[\,\underline{\mathbb{M}}\,][\underline{\mathbb{T}}(\omega)]\}\;d\omega \quad , \tag{2}$$

where $\Re e$ is the real part of complex number and where $[\underline{\mathbb{T}}(\omega)]^* = \overline{[\underline{\mathbb{T}}(\omega)]}^T$ is the adjoint matrix. It should be noted that $[\underline{\mathbb{E}}_B]$ depends on MF band B, but does not depend on the given load vector. For energy matrix $[\underline{\mathbb{E}}_B]$, the eigenvalue problem is written as $[\underline{\mathbb{E}}_B]\,\underline{\mathbf{P}} = \underline{\lambda}\,\underline{\mathbf{P}}$. The normalization condition of the real eigenvectors is chosen as $\|\underline{\mathbf{P}}\|^2 =<\underline{\mathbf{P}}\,,\underline{\mathbf{P}}>= 1$. The dominant eigensubspace of dimension $n << m$ is spanned by the real eigenvectors $\underline{\mathbf{P}}_1, \underline{\mathbf{P}}_2, \ldots, \underline{\mathbf{P}}_n$ associated with the n highest eigenvalues $\underline{\lambda}_1 \geq \underline{\lambda}_2 \geq \ldots \geq \underline{\lambda}_n$. Introducing the rectangular $(m \times n)$ real matrix $[\underline{P}_n^B] = [\underline{\mathbf{P}}_1 \ldots, \underline{\mathbf{P}}_n]$ whose columns are constituted of eigenvectors $\underline{\mathbf{P}}_1, \ldots, \underline{\mathbf{P}}_n$ and introducing the diagonal square $(n \times n)$ real matrix $[\underline{\Lambda}_n]$ whose diagonal entries are $\underline{\lambda}_1, \ldots, \underline{\lambda}_n$, the eigenvalue problem allowing the dominant eigenspace of energy matrix $[\underline{\mathbb{E}}_B]$ to be constructed is written as

$$[\underline{\mathbb{E}}_B]\,[\underline{P}_n^B] = [\underline{P}_n^B]\,[\underline{\Lambda}_n] \quad , \quad [\underline{P}_n^B]^T\,[\underline{P}_n^B] = [I_n] \quad , \tag{3}$$

where $[I_n]$ is the $(n \times n)$ identity matrix. Matrix $[\underline{P}_n^B]$ is calculated by solving Eq. (3). For the computation, matrix $[\underline{\mathbb{E}}_B]$ is not directly calculated by Eq. (2) using a direct calculation of matrix-valued frequency response function $\{[\underline{\mathbb{T}}(\omega)], \omega \in B\}$. An indirect procedure based on

the subspace iteration method coupled with a solution method in the time domain (see Soize 1998) is used. Such a procedure does not use the knowledge of complex matrix $[\underline{\mathbb{I}}(\omega)]$ which is generally full.

The mean reduced matrix model is obtained in projecting the mean ¿nite element model de¿ned by Eq. (1) on the dominant eigensubspace of energy matrix $[\underline{\mathbb{E}}_B]$. The approximation $\underline{\mathbf{y}}^n(\omega)$ of $\underline{\mathbf{y}}(\omega)$ is then written as

$$\underline{\mathbf{y}}^n(\omega) = [\underline{P}_n^B]\, \underline{\mathbf{q}}^n(\omega) \quad , \tag{4}$$

in which, for all ω ¿xed in B, the $\mathbb{C}^n$-vector $\underline{\mathbf{q}}^n(\omega)$ of the generalized coordinates is the unique solution of the mean reduced matrix equation,

$$\left(-\omega^2\, [\,\underline{M}_n\,] + i\omega\, [\underline{D}_n(\omega)] + [\underline{K}_n(\omega)]\,\right)\, \underline{\mathbf{q}}^n(\omega) = \underline{\mathbf{F}}^n(\omega) \quad , \quad \omega \in B \quad , \tag{5}$$

with $\underline{\mathbf{F}}^n(\omega) = [\underline{P}_n^B]^T\, \underline{\mathbf{f}}(\omega) \in \mathbb{C}^n$ and where the mean generalized mass, damping and stiffness matrices are the positive-de¿nite symmetric $(n \times n)$ real full matrices such that $[\,\underline{M}_n\,] = [\underline{P}_n^B]^T\, [\,\underline{\mathbb{M}}\,]\, [\underline{P}_n^B]$, $[\underline{D}_n(\omega)] = [\underline{P}_n^B]^T\, [\underline{\mathbb{D}}(\omega)]\, [\underline{P}_n^B]$ and $[\underline{K}_n(\omega)] = [\underline{P}_n^B]^T\, [\underline{\mathbb{K}}(\omega)]\, [\underline{P}_n^B]$.

Nonparametric model of random uncertainties in the MF band

Using the idea of the nonparametric model of random uncertainties introduced by (Soize 2000), the principle of construction of the nonparametric model of random uncertainties in the MF band consists in modeling the generalized mass, damping and stiffness matrices of the mean reduced model de¿ned by Eqs. (4) and (5) by random matrices $[\mathbf{M}_n]$, $[\mathbf{D}_n(\omega)]$ and $[\mathbf{K}_n(\omega)]$ whose probability model has to be de¿ned. In the MF band, the nonparametric model of random uncertainties is then written as

$$\mathbf{Y}^n(\omega) = [\underline{P}_n^B]\, \mathbf{Q}^n(\omega) \quad , \tag{6}$$

in which, for all ω ¿xed in B, the $\mathbb{C}^n$-valued random variable $\mathbf{Q}^n(\omega)$ of the random generalized coordinates is the unique solution of the random reduced matrix equation,

$$\left(-\omega^2\, [\mathbf{M}_n] + i\omega\, [\mathbf{D}_n(\omega)] + [\mathbf{K}_n(\omega)]\,\right)\, \mathbf{Q}^n(\omega) = \underline{\mathbf{F}}^n(\omega) \quad , \quad \omega \in B \quad . \tag{7}$$

The probability model of these random matrices is de¿ned (see Soize 2000 & 2001) as

$$[\mathbf{M}_n] = [\underline{L}_{M_n}]^T\, [\mathbf{G}_{M_n}]\, [\underline{L}_{M_n}] \quad , \tag{8}$$

$$[\mathbf{D}_n(\omega)] = [\underline{L}_{D_n}(\omega)]^T\, [\mathbf{G}_{D_n}]\, [\underline{L}_{D_n}(\omega)] \quad , \tag{9}$$

$$[\mathbf{K}_n(\omega)] = [\underline{L}_{K_n}(\omega)]^T\, [\mathbf{G}_{K_n}]\, [\underline{L}_{K_n}(\omega)] \quad , \tag{10}$$

in which the upper triangular $(n \times n)$ real matrices $[\underline{L}_{M_n}]$, $[\underline{L}_{D_n}(\omega)]$ and $[\underline{L}_{K_n}(\omega)]$ correspond to the Chowlesky factorization $[\,\underline{M}_n\,] = [\underline{L}_{M_n}]^T\,[\underline{L}_{M_n}]$, $[\underline{D}_n(\omega)] = [\underline{L}_{D_n}(\omega)]^T\,[\underline{L}_{D_n}(\omega)]$ and $[\underline{K}_n(\omega)] = [\underline{L}_{K_n}(\omega)]^T\,[\underline{L}_{K_n}(\omega)]$ of positive-de¿nite symmetric $(n \times n)$ real matrices $[\,\underline{M}_n\,]$, $[\underline{D}_n(\omega)]$ and $[\underline{K}_n(\omega)]$ respectively. From the theory developed, it is deduced that random matrices $[\mathbf{G}_{M_n}]$, $[\mathbf{G}_{D_n}]$ and $[\mathbf{G}_{K_n}]$ are independent and that their dispersions are controlled by the positive real parameters δ_M, δ_D and δ_K which are independent of dimension n and do not depend on frequency ω. The independence property is due to the use of the maximum entropy principle for which no information concerning the correlation tensor between the random matrices is available. If A_n represents M_n, D_n or K_n, then random matrix $[\mathbf{G}_{A_n}]$, with dispersion parameter δ_A, is such that $[\mathbf{G}_{A_n}] = [\mathbf{L}_{A_n}]^T\,[\mathbf{L}_{A_n}]$. The matrix $[\mathbf{L}_{A_n}]$ is an upper triangular random $(n \times n)$ real matrix such that the random variables $\{[\mathbf{L}_{A_n}]_{jj'}, j \leq j'\}$ are independent and such that

(1) for $j < j'$, real-valued random variable $[\mathbf{L}_{A_n}]_{jj'}$ is written as $[\mathbf{L}_{A_n}]_{jj'} = \sigma_n U_{jj'}$ in which $\sigma_n = \delta_A (n+1)^{-1/2}$ and where $U_{jj'}$ is a real-valued Gaussian random variable with zero mean and variance equal to 1;

(2) for $j = j'$, positive-valued random variable $[\mathbf{L}_{A_n}]_{jj}$ is written as $[\mathbf{L}_{A_n}]_{jj} = \sigma_n \sqrt{2V_j}$ in which σ_n is de¿ned above and where V_j is a positive-valued gamma random variable whose probability density function $p_{V_j}(v)$ with respect to dv is written as

$$p_{V_j}(v) = \mathbb{1}_{\mathbb{R}^+}(v)\{\Gamma(\frac{n+1}{2\delta_A^2} + \frac{1-j}{2})\}^{-1}\; v^{\frac{n+1}{2\delta_A^2} - \frac{1+j}{2}}\; e^{-v} \quad . \tag{11}$$

It should be noted that the probability model of random matrix $[\mathbf{G}_{A_n}]$ is mathematically well de¿ned, in particular when dimension n goes to in¿nity (see Soize 2001).

Convergence analysis of the random medium-frequency response

For every $\omega \in B$, the random response $\mathbf{Y}^n(\omega)$ of the stochastic system subjected to the given deterministic load is the $\mathbb{C}^n$-valued second-order random variable which is the solution of Eqs. (6) and (7). The norm of the $\mathbb{C}^n$-valued second-order stochastic process $\{\mathbf{Y}^n(\omega), \omega \in B\}$ is de¿ned by $|||\mathbf{Y}^n||| = \left(E\{\int_B \|\mathbf{Y}^n(\omega)\|^2\, d\omega\}\right)^{1/2}$. From Eqs. (3) and (6), it can be deduced that $|||\mathbf{Y}^n||| = |||\mathbf{Q}^n|||$. Consequently, the mean-square convergence with respect to n of the sequence of stochastic processes $\{\mathbf{Y}^n(\omega), \omega \in B\}_n$ can be studied considering the mapping $n \mapsto |||\mathbf{Q}^n|||$.

Con¿dence region of the random acceleration for the stochastic system subjected to the given deterministic load

Let $\mathbf{Y}^n(\omega) = (Y_1^n(\omega), \ldots, Y_m^n(\omega))$ be the random response of the stochastic system constructed with the nonparametric model of random uncertainties and subjected to the given deterministic load vector $\underline{\mathbf{f}}(\omega)$. Let $S(\omega) = |-\omega^2 Y_j^n(\omega)|$ be the random response corresponding to the acceleration of DOF j. Let $\mathrm{dB}(\omega)$ be the random variable de¿ned by $\mathrm{dB}(\omega) = \log_{10}(S(\omega))$. For a given probability level P_c (for instance $P_c = 0.95$), the con¿dence region of the stochastic process $\{\mathrm{dB}(\omega), \omega \in B\}$ is de¿ned by

$$\mathrm{Proba}\{\mathrm{dB}^-(\omega) < \mathrm{dB}(\omega) \leq \mathrm{dB}^+(\omega)\} \geq P_c \quad , \tag{12}$$

in which the lower and upper envelopes $\mathrm{dB}^-(\omega)$ and $\mathrm{dB}^+(\omega)$ are de¿ned by

$$\mathrm{dB}^+(\omega) = \log_{10}\left(E\{S(\omega)\} + \sigma(\omega)/\sqrt{1-P_c}\right) \ , \ \mathrm{dB}^-(\omega) = 2\,\mathrm{dB}_0(\omega) - \mathrm{dB}^+(\omega) \quad , \tag{13}$$

in which $\mathrm{dB}_0(\omega) = \log_{10}(E\{S(\omega)\})$ and where $\sigma(\omega)$ is the standard deviation of $S(\omega)$. The standard deviations are usually estimated by using the Monte Carlo numerical simulation.

RANDOM ENERGY MATRIX RELATED TO A MEDIUM-FREQUENCY BAND AND ITS RANDOM EIGENVALUES

Random energy matrix

It is interesting to introduce the approximation $[\mathbb{E}_B^n]$ of order n of the random energy matrix relating to MF band B, which is independent of any given load. This is a random positive-semide¿nite symmetric $(m \times m)$ real matrix de¿ned (see Eq. (2)) by

$$[\mathbb{E}_B^n] = [\underline{P}_n^B]\,[\mathbf{E}_n]\,[\underline{P}_n^B]^T \quad , \quad [\mathbf{E}_n] = \frac{1}{\pi}\int_B \omega^2\, \Re e\left\{[\mathbf{T}_n(\omega)]^*[\mathbf{M}_n][\mathbf{T}_n(\omega)]\right\} d\omega \quad , \tag{14}$$

where $[\mathbf{T}_n(\omega)]$ is the random symmetric $(n \times n)$ complex matrix de¿ned by

$$[\mathbf{T}_n(\omega)] = \left(-\omega^2\,[\mathbf{M}_n] + i\omega\,[\mathbf{D}_n(\omega)] + [\mathbf{K}_n(\omega)]\right)^{-1} \quad , \tag{15}$$

and where $[\mathbf{E}_n]$ is a random positive-de¿nite symmetric $(n \times n)$ real matrix.

Random eigenvalues of the random energy matrix and the random trace

The random eigenvalue problem associated with random energy matrix $[\mathbf{E}_n]$ is written as

$$[\mathbf{E}_n]\,[\mathbf{\Psi}_n] = [\mathbf{\Psi}_n]\,[\mathbf{\Lambda}] \quad , \quad [\mathbf{\Psi}_n]^T\,[\mathbf{\Psi}_n] = [\mathbf{\Psi}_n]\,[\mathbf{\Psi}_n]^T = [I_n] \quad a.s. \quad , \tag{16}$$

in which *a.s.* means *almost surely*, where $[I_n]$ is the $(n \times n)$ identity matrix, where $[\mathbf{\Lambda}]$ is the diagonal $(n \times n)$ matrix of the random eigenvalues and where$[\mathbf{\Psi}_n]$ is the $(n \times n)$ matrix constituted of the random eigenvectors. Since $[\mathbf{E}_n]$ is a random positive-de¿nite symmetric $(n \times n)$ real matrix, (1) the random eigenvalues are positive-valued random variables and the order statistics $\Lambda_1 \geq \ldots \geq \Lambda_n > 0$ is then introduced, (2) the associated random eigenvectors is an orthonormal systems of random vectors for the Euclidean inner product. We then have

$$[\mathbf{E}_n] = [\mathbf{\Psi}_n]\,[\mathbf{\Lambda}]\,[\mathbf{\Psi}_n]^T \quad . \tag{17}$$

Let $\mathcal{E}_n$ be the trace of random energy matrix $[\mathbb{E}_B^n]$. From Eqs. (3),(14) and (16), it can be deduced that $\mathcal{E}_n$ is a positive-valued random variable which is such that

$$\mathcal{E}_n = \text{tr}\{[\mathbb{E}_B^n]\} = \text{tr}\{[\mathbf{E}_n]\} = \sum_{\alpha=1}^{n} \Lambda_\alpha \quad . \tag{18}$$

The probability density function of positive-valued random variable $\mathcal{E}_n$ is the mapping $e \mapsto p_{\mathcal{E}_n}(e)$ de¿ned in $\mathbb{R}^+$ with values in $\mathbb{R}^+$. In the next Section, the convergence with respect to n of the sequence of probability density functions $\{e \mapsto p_{\mathcal{E}_n}(e)\}_n$ is studied. The moments of the random eigenvalues $\Lambda_1, \ldots, \Lambda_n$ and the probability density function $p_{\mathcal{E}_n}$ are usually estimated by using the Monte Carlo numerical simulation. It should be noted that, even if the system is lightly damped, then random eigenvectors $[\mathbf{\Psi}_n]$ differ from the random normal modes (see Soize 1998). In addition, we are interested in investigating the random total energy $\mathcal{E}_n$ of the system and not in investigating the individual random eigenvalues $\Lambda_1, \Lambda_2, \ldots$, which have no real physical meaning in the medium-frequency range.

NUMERICAL EXAMPLE

Mean model of the dynamical system and its mean ¿nite element model

The mean model of the nonhomogeneous dynamical system is constituted of a thin plate with two attached point masses and two springs. The thin plate is rectangular, homogeneous, isotropic and

located in the plane (Ox_1, Ox_2) of a Cartesian coordinate system $(Ox_1x_2x_3)$, in bending mode (the outplane displacement is x_3), with constant thickness $0.001\,m$, width along Ox_2 is $0.40\,m$, length along Ox_1 is $0.50\,m$, mass density $7800\,kg/m^3$, Young's modulus $2.1 \times 10^{11}\,N/m^2$ and Poisson ratio 0.29 . This plate is simply supported on 3 edges and free on the fourth edge corresponding to $x_2 = 0$ (see Figure 1). There are two point masses having a mass $10\,kg$ and $6\,kg$ located at points $(0.15, 0.15, 0)$ and $(0.31, 0.20, 0)$ respectively, and two springs having a stiffness coef¿cient $k = 1.2090 \times 10^9\,N/m$ and $k = 7.0893 \times 10^8\,N/m$ located at points $(0.15, 0.15, 0)$ and $(0.31, 0.20, 0)$ respectively.

The mean ¿nite element model of the plate is composed of a regular rectangular mesh with a constant step size of $0.01\,m$ in x_1 and x_2 (41 nodes in the width, 51 nodes in the length), each ¿nite element being a 4-node square plate element. There are 2000 ¿nite elements and $m = 6009$ degrees of freedom (x_3-translations and x_1- and x_2-rotations). The two ¿rst eigenfrequencies of the mean undamped dynamical system, calculated with the mean ¿nite element model, are $27.73\,Hz$ and $57.35\,Hz$. There are 82 eigenfrequencies in the frequency band $[0\,,1400]\,Hz$ and respectively, 13, 20 and 11 eigenfrequencies in the frequency bands $[1400\,,1600]\,Hz$, $[1600\,,1900]\,Hz$ and $[1900\,,2100]\,Hz$. The medium-frequency band of analysis is de¿ned as $B = 2\pi \times [1600\,,1900]$ rad/s. In the frequency domain, for all $\omega \in B$, the given deterministic load vector $\underline{\mathbf{f}}(\omega) \in \mathbb{C}^m$ is written as $\underline{\mathbf{f}}(\omega) = \mathbf{Z}$ in which the spatial part $\mathbf{Z} = (Z_1, \ldots, Z_m) \in \mathbb{R}^m$ is independent of ω and is such that $Z_j = 0$ for all j in $\{1, \ldots, m\}$ except for the nine DOFs in x_3-translations corresponding to the nodes whose (x_1, x_2) coordinates are $(0.21, 0.23)$, $(0.21, 0.24)$, $(0.21, 0.25)$, $(0.22, 0.23)$, $(0.22, 0.24)$, $(0.22, 0.25)$, $(0.23, 0.23)$, $(0.23, 0.24)$ and $(0.23,\ 0.25)$, for which $Z_j = 1$. Damping matrix $[\,\underline{\mathbb{D}}(\omega)]$ of the mean ¿nite element model depends on the frequency and is written as $[\,\underline{\mathbb{D}}(\omega)] = 2\,\underline{\xi}\,\omega\,[\,\underline{\mathbb{M}}\,]$ in which $\underline{\xi} = 0.002$. In the system, the observations are the three DOF numbers j_{obs1}, j_{obs2} and j_{obs3} corresponding to the x_3-translation of the mesh node located at points of coordinates $(0.22, 0.24, 0)$ (excitation point), $(0.31, 0, 0)$ (free edge point) and $(0.37, 0.15, 0)$ (inside point) respectively.

Reference solution for the mean model on a broad frequency band

For the mean model, the reference solution is obtained by solving Eq. (1) with the direct frequency-by-frequency method with 2100 sample points in the frequency band $[0\,,2100]$ Hertz. Figure 2 shows the graph of the function $\omega \mapsto \log_{10}(\| -\omega^2 \underline{\mathbf{y}}(\omega)\|)$. In this ¿gure, it can be seen

that frequency band $B = 2\pi \times [1600\,,1900]\,rad/s$ belongs to the medium-frequency range.

Mean reduced matrix model on MF band B

The dominant eigensubspace of energy matrix $[\underline{\mathbb{E}}_B]$ relating to the MF band [1600 , 1900] Hz is calculated by solving the symmetric eigenvalue problem de¿ned by Eq. (3) as explained above. Figure 3 shows the graph of the function $\alpha \mapsto \underline{\lambda}_\alpha$ in which $\underline{\lambda}_1 > \ldots > \underline{\lambda}_{50}$ are the 50 highest eigenvalues of $[\underline{\mathbb{E}}_B]$. It can be seen the strong decrease of eigenvalues when the order of the eigenvalues is greater than 20 allowing the construction of a mean reduced matrix model having a small dimension.

Convergence analysis of the stochastic system

We consider the stochastic dynamical system in MF band B for which the dispersion parameters which control the mass, damping and stiffness uncertainties are such that $\delta_M = \delta_D = \delta_K = 0.02$. The Monte Carlo numerical simulation is carried out with n_s realizations denoted by $\theta_1, \ldots, \theta_{n_s}$. For the random response of the stochastic system subjected to given deterministic load vector $\underline{\mathbf{f}}(\omega)$ over MF band B, the norm $|||\mathbf{Y}^n||| = |||\mathbf{Q}^n|||$ is estimated by $\text{Conv}(n_s, n) = \left\{ \frac{1}{n_s} \sum_{k=1}^{n_s} \int_B \|\mathbf{Q}^n(\omega, \theta_k)\|^2 \, d\omega \right\}^{1/2}$. For the random trace $\mathcal{E}_n = \text{tr}\{[\mathbb{E}_B^n]\}$ of random energy matrix $[\mathbb{E}_B^n]$ relating to MF band B, which is independent of any given load, the probability density function $e \mapsto p_{\mathcal{E}_n}(e)$ of random variable $\mathcal{E}_n$ is estimated by the usual mathematical statistics.

Figures 4 and 5 concern the convergence of $|||\mathbf{Y}^n|||$ with respect to dimension n of the stochastic reduced matrix model and to the number n_s of realizations used in the Monte Carlo numerical simulation. For $n = 35$, Figure 4 displays the graph of the function $n_s \mapsto \log_{10}\{\text{Conv}(n_s, n)\}$. For $n_s = 10000$, Figure 5 shows the graph of the function $n \mapsto \log_{10}\{\text{Conv}(n_s, n)\}$. It can be seen that mean square convergence is reached for $n \geq 35$ and $n_s \geq 5000$.

Figures 6, 7 and 8 are relating to convergence of the stochastic dynamical system with respect to dimension n of the stochastic reduced matrix model, in terms of random variable $\mathcal{E}_n$ which is intrinsic and independent of any given load. The calculations are carried out with $n_s = 10000$. Figure 6 displays two curves: (1) for the mean dynamical system, the graph of the function $n \mapsto \underline{\mathcal{E}}_n$ (triangle symbols) of the trace $\underline{\mathcal{E}}_n$ of energy matrix $[\underline{\mathbb{E}}_B^n]$ relating to MF band B, (2) for

the stochastic dynamical system, the graph of the mean function $n \mapsto E\{\mathcal{E}_n\}$ (circle symbols) of random variable $\mathcal{E}_n$. For the stochastic dynamical system, Figure 7 shows the graph of the standard deviation function $n \mapsto \sigma_{\mathcal{E}_n}$ (circle symbols) of random variable $\mathcal{E}_n$. Figure 8 displays the graphs of the probability density functions $\{e \mapsto p_{\mathcal{E}_n}(e)\}_n$ of random variable $\mathcal{E}_n$ for $n =$ 5,15,20,25,35 (thin solid lines) and for $n = 45$ (thick solid line). Figures 6 to 8 show that convergence is effectively reach for $n \geq 35$, independently of any given load.

Random response of the stochastic system subjected to a given deterministic load

We consider the random response of the stochastic dynamical system with $\delta_M = \delta_D = \delta_K = 0.02$ and subjected to given deterministic load vector $\underline{\mathbf{f}}(\omega)$ over MF band B. The calculations are carried out for $n = 35$ and $n_s = 10000$. Figures 9-a to 9-c are relating to DOF numbers j_{obs1} (excitation point), j_{obs2} (free edge point) and j_{obs3} (inside point), respectively. Each ¿gure displays the graphs relating to the con¿dence region of the random acceleration $\text{dB}(\omega)$ for the probability level 0.95 and over MF band B.

Random energy matrix relating to an MF band and its random eigenvalues

The stochastic dynamical system with $\delta_M = \delta_D = \delta_K = 0.02$ is considered again and we are interested in the random eigenvalues Λ_α of random energy matrix $[\mathbb{E}_B^n]$ relating to MF band B and in the random trace $\mathcal{E}_n$ of $[\mathbb{E}_B^n]$. The calculations are carried out with $n = 35$ and $n_s = 10000$. Figure 10 displays the graph of the mean function $\alpha \mapsto E\{\Lambda_\alpha\}$ of random eigenvalues Λ_α. It should be noted that this graph looks like to the graph shows in Figure 3, that is coherent with Figure 6 because $\underline{\mathcal{E}}_n = \text{tr}\{[\underline{\mathbb{E}}_B^n]\} = \sum_{\alpha \geq 1} \underline{\lambda}_\alpha$ and $\mathcal{E}_n = \text{tr}\{[\mathbb{E}_B^n]\} = \text{tr}\{[\mathbf{E}_B^n]\} = \sum_{\alpha \geq 1} \Lambda_\alpha$. Figure 11 shows the graph of the standard deviation function $\alpha \mapsto \log_{10}(\sigma_{\Lambda_\alpha})$ of random eigenvalues Λ_α. It should be noted that the standard deviation is maximum for the random eigenvalues whose mean values correspond to the strong decrease in Figure 10. Figure 12 displays the graph of the probability density function $e \mapsto p_{\mathcal{E}_n}(e)$ of positive-valued random variable $\mathcal{E}_n$ which is not Gaussian and which is (almost) unimodal.

Sensitivity analysis of the random energy matrix relating to an MF band with respect to the dispersion parameters

We consider the random trace $\mathcal{E}_n$ of random energy matrix $[\mathbb{E}_B^n]$ relating to MF band B for the stochastic dynamical system whose dispersion parameters which control the mass, damping and stiffness uncertainties are δ_M, δ_D and δ_K. The calculations are performed with $n = 35$ and $n_s = 5000$. Figure 13 displays the graphs of the normalized mean functions $\delta_M \mapsto E\{\mathcal{E}_n\}/\underline{\mathcal{E}}_n$ with $\delta_D = \delta_K = 0$ (plus symbol), $\delta_D \mapsto E\{\mathcal{E}_n\}/\underline{\mathcal{E}}_n$ with $\delta_M = \delta_K = 0$ (triangle symbol) and $\delta_K \mapsto E\{\mathcal{E}_n\}/\underline{\mathcal{E}}_n$ with $\delta_M = \delta_D = 0$ (circle symbol). Figure 14 shows the graphs of the normalized standard deviation functions $\delta_M \mapsto \sigma_{\mathcal{E}_n}/\underline{\mathcal{E}}_n$ with $\delta_D = \delta_K = 0$ (plus symbol), $\delta_D \mapsto \sigma_{\mathcal{E}_n}/\underline{\mathcal{E}}_n$ with $\delta_M = \delta_K = 0$ (triangle symbol) and $\delta_K \mapsto \sigma_{\mathcal{E}_n}/\underline{\mathcal{E}}_n$ with $\delta_M = \delta_D = 0$ (circle symbol). Figure 13 and 14 show that the effects of damping uncertainties are less that the effects of stiffness or mass uncertainties and, in addition, that the effects of stiffness uncertainties are equivalent to the effects of mass uncertainties.

Sensitivity analysis of the random response of stochastic system subjected to a given deterministic load with respect to the dispersion parameters

We consider the stochastic dynamical system subjected to given deterministic load vector $\underline{\mathbf{f}}(\omega)$ over MF band B. The calculations are performed for $n = 35$ and $n_s = 5000$. Figures 15-a to 15-f are relating to the stochastic response for DOF number j_{obs3} (inside point) as a function of dispersion parameters δ_M, δ_D and δ_K. Each ¿gure displays the graphs relating to the con¿dence region of the random acceleration $\text{dB}(\omega)$ for the probability level 0.95 and over MF band B. Figures 15-a to 15-d show that the effects of stiffness uncertainties are equivalent to the effects of mass uncertainties. Figures 15-e and 15-f show that the effects of damping uncertainties are relatively small and are less that the effects of stiffness or mass uncertainties. These results are coherent with those obtained in Figures 13 and 14. The conclusions are the same for the other DOF numbers j_{obs2} (free edge point) and j_{obs3} (inside point).

Sensitivity analysis of the probability distribution of the trace of the random energy matrix relating to an MF band with respect to the dispersion parameters

We consider the probability distribution of the random trace $\mathcal{E}_n$ of random energy matrix $[\mathbb{E}_B^n]$ relating to MF band B for the stochastic dynamical system whose dispersion parameters are δ_M, δ_D and δ_K. The calculations are performed with $n = 35$ and $n_s = 20000$. Figures 16-a to 16-e display the graph of the probability density functions $e \mapsto p_{\mathcal{E}_n}(e)$ of random variable $\mathcal{E}_n$ for

several values of δ_M, δ_D and δ_K. For $\delta_M = \delta_D = 0$, Figures 16-a, 16-b and 16-c correspond to $\delta_K = 0.02$, 0.3 and 0.5, respectively. It should be noted that these results are similar to the results corresponding to $\delta_D = \delta_K = 0$ and $\delta_M = 0.02$, 0.3 and 0.5, respectively. These ¿gures show that the probability density function of random variable $\mathcal{E}_n$ becomes multimodal when the value of dispersion parameter δ_K (or δ_M) increases. In opposite, Figures 16-d and 16-e show that the probability density function of random variable $\mathcal{E}_n$ remains unimodal when the value of dispersion parameter δ_D increases.

Stability of the stochastic reponse with respect to the bandwidth of the MF band

This section is devoted to the analysis of the proposed nonparametric model of random uncertainties in the medium-frequency range with respect to the bandwidth of the MF band. We then consider the stochastic dynamical system with $\delta_M = \delta_D = \delta_K = 0.02$ and subjected to given deterministic load vector $\underline{\mathbf{f}}(\omega)$, over three overlapped MF bands $B = 2\pi \times [1600\,,1900]\, rad/s$, $B' = 2\pi \times [1400\,,1900]\, rad/s$ and $B'' = 2\pi \times [1600\,,2100]\, rad/s$ such that $B \subset B'$, $B \subset B''$ and $B = B' \cap B''$. Let $\{\mathbf{Y}_B^n(\omega), \omega \in B\}$, $\{\mathbf{Y}_B^{n'}(\omega), \omega \in B'\}$ and $\{\mathbf{Y}_B^{n''}(\omega), \omega \in B''\}$ be the solutions of the stochastic dynamical system subjected to the given deterministic load de¿ned on MF bands B, B' and B'' respectively. The calculations are performed with $n_s = 10000$ and, with $n = 35$ for band B and with $n' = n'' = 58$ for bands B' and B''. Figures 17-a, 17-b and 17-c are relating to DOF numbers j_{obs1} (excitation point), j_{obs2} (free edge point) and j_{obs3} (inside point), respectively. Each ¿gure displays the graphs relating to the con¿dence region of the random acceleration $\text{dB}(\omega)$ for the probability level 0.95 and over MF bands B, B' and B''. These ¿gures show that the con¿dence regions coincide over MF band B with a good accuracy.

CONCLUSIONS

We have presented a novel approach for modeling random uncertainties in the medium-frequency dynamics. For the mechanical system considered in the numerical example, the major conclusions are the following:

(1) The convergence properties with respect to the dimension of the random reduced matrix model have been veri¿ed (a) for the random response of the stochastic system subjected to a

given load and (b) for the probability density function of the random trace of the random energy matrix which is intrinsic and which is independent of any given load.

(2) For a given medium-frequency band, a sensitivity analysis with respect to the dispersion parameters has been performed for the random energy matrix of the stochastic system and for the random response of this stochastic system subjected to a given deterministic load. The results show that, in the medium-frequency band, (a) the effects of damping uncertainties are less that the effects of stiffness or mass uncertainties (b) the effects of stiffness uncertainties are equivalent to the effects of mass uncertainties, (c) the probability density function of random trace of the random energy matrix is not Gaussian and becomes multimodal when the dispersion-parameter value of the stiffness (or of the mass) increases; in opposite, the probability density function of the random trace remains unimodal when the damping dispersion parameter increases.

(3) For the medium-frequency range, the proposed probabilistic modeling of random uncertainties is coherent with respect to the bandwith of the MF band of analysis.

APPENDIX. REFERENCES

Argyris, J., and Mlejnek, H. P. (1991). *Dynamics of Structures*. North Holland, Amsterdam.

Cameron, R. H., and Martin, W. T. (1947). "The orthogonal development of nonlinear functionals in series of Fourier-Hermite functionals". *Ann. Math*, **48**, 385-392.

Clough, R.W., and Penzien, J. (1975). *Dynamics of Structures*. McGraw-Hill, New York.

Ghanem, R. (1999). "Ingredients for a general purpose stochastic ¿nite elements formulation". *Computer Methods in Applied Mechanics and Engineering*, **168**, 19-34.

Ghanem, R., and Spanos, P. D. (1991). *Stochastic Finite Elements: A spectral Approach*. Springer-Verlag, New York.

Ghanem, R., and Sarkar, A. (2003). "Reduced models for the medium-frequency dynamics of stochastic systems". *J. Acoust. Soc. Am.*, to appear.

Guikhman, L., and Skorokhod, A. V. (1979). *The Theory of Stochastic Processes*. Springer verlag, Berlin.

Ohayon, R., and Soize, C. (1998). *Structural Acoustics and Vibration*. Academic Press, San Diego.

Soize, C. (1998). "Reduced Models in the Medium-Frequency Range for General Dissipative Structural-Dynamics Systems". *European Journal of Mechanics, A/Solids*, **17**(4), 657-685.

Soize, C. (2000). "A Nonparametric Model of Random Uncertainties for Reduced Matrix Models in Structural Dynamics". *Probabilistic Engineering Mechanics*, **15**(3), 277-294.

Soize, C. (2001). "Maximum Entropy Approach for Modeling Random Uncertainties in Transient Elastodynamics". *J. Acoust. Soc. Am.*, **109**(5), 1979-1996.

LEGENDS ACCOMPANYING EACH FIGURE

FIG. 1. De¿nition of the mean dynamical system.

FIG. 2. Graph of function $\nu \mapsto \log_{10}(\| - (2\pi\nu)^2 \underline{\mathbf{y}}(2\pi\nu)\|)$ relating to the mean model over the broad frequency band [0 , 2100] Hertz (horizontal axis).

FIG. 3. Graph of function $\alpha \mapsto \underline{\lambda}_\alpha$ for the mean model over the MF band [1600 , 1900] Hz.

FIG. 4. Graph of function $n_s \mapsto \log_{10}\{\text{Conv}(n_s, n)\}$ for the stochastic dynamical system with $n = 35$ and over the MF band $[1600, 1900]$ Hz.

FIG. 5. Graph of function $n \mapsto \log_{10}\{\text{Conv}(n_s, n)\}$ for the stochastic dynamical system with $n_s = 10000$ and over the MF band $[1600, 1900]$ Hz.

FIG. 6. Graph of function $n \mapsto \underline{\mathcal{E}}_n$ (triangle symbol) for the mean model and graph of function $n \mapsto E\{\mathcal{E}_n\}$ (circle symbol) for the stochastic dynamical system over the MF band $[1600, 1900]$ Hz.

FIG. 7. Graph of function $n \mapsto \sigma_{\mathcal{E}_n}$ (circle symbol) for the stochastic dynamical system over the MF band $[1600, 1900]$ Hz.

FIG. 8. Graphs of probability density functions $\{e \mapsto p_{\mathcal{E}_n}(e)\}_n$ for $n =$ 5,15,20,25,35 (thin solid lines) and for $n = 45$ (thick solid line) for the stochastic dynamical system over the MF band $[1600, 1900]$ Hz.

FIG. 9-a. DOF number j_{obs1} (excitation point).

FIG. 9-b. DOF number j_{obs2} (free edge point).

FIG. 9-c. DOF number j_{obs3} (inside point).

FIG. 9-a-b-c. Con¿dence region of the random acceleration dB (vertical axis) for DOF numbers j_{obs1}, j_{obs2} and j_{obs3} over the MF band $[1600, 1900]$ Hz (horizontal axis): deterministic response of the mean model (mid irregular thin solid line), mean value of the random response of the stochastic model (mid regular thin solid line), lower and upper envelopes of the con¿dence region corresponding to the probability level 0.95 (lower and upper thick solid lines).

FIG. 10. Graph of the mean function $\alpha \mapsto E\{\Lambda_\alpha\}$ for the stochastic dynamical system over the MF band $[1600, 1900]$ Hz.

FIG. 11. Graph of the standard deviation function $\alpha \mapsto \log_{10}(\sigma_{\Lambda_\alpha})$ for the stochastic dynamical system over the MF band $[1600, 1900]$ Hz.

FIG. 12. Graph of the probability density function $e \mapsto p_{\mathcal{E}_n}(e)$ for the stochastic dynamical system over the MF band $[1600, 1900]$ Hz.

FIG. 13. Graphs of the normalized mean functions $\delta_M \mapsto E\{\mathcal{E}_n\}/\underline{\mathcal{E}}_n$ with $\delta_D = \delta_K = 0$ (plus symbol), $\delta_D \mapsto E\{\mathcal{E}_n\}/\underline{\mathcal{E}}_n$ with $\delta_M = \delta_K = 0$ (triangle symbol) and $\delta_K \mapsto E\{\mathcal{E}_n\}/\underline{\mathcal{E}}_n$ with $\delta_M = \delta_D = 0$ (circle symbol), for the stochastic dynamical system over the MF band $[1600, 1900]$ Hz.

FIG. 14. Graphs of the normalized standard deviation functions $\delta_M \mapsto \sigma_{\mathcal{E}_n}/\underline{\mathcal{E}}_n$ with $\delta_D = \delta_K = 0$ (plus symbol), $\delta_D \mapsto \sigma_{\mathcal{E}_n}/\underline{\mathcal{E}}_n$ with $\delta_M = \delta_K = 0$ (triangle symbol) and $\delta_K \mapsto \sigma_{\mathcal{E}_n}/\underline{\mathcal{E}}_n$ with $\delta_M = \delta_D = 0$ (circle symbol), for the stochastic dynamical system over the MF band $[1600, 1900]$ Hz.

FIG. 15-a. $\delta_M = 0, \delta_D = 0, \delta_K = 0.02$.

FIG. 15-b. $\delta_M = 0.02, \delta_D = 0, \delta_K = 0$.

FIG. 15-c. $\delta_M = 0, \delta_D = 0, \delta_K = 0.5$.

FIG. 15-d. $\delta_M = 0.5, \delta_D = 0, \delta_K = 0$.

FIG. 15-e. $\delta_M = 0, \delta_D = 0.02, \delta_K = 0$.

FIG. 15-f. $\delta_M = 0, \delta_D = 0.5, \delta_K = 0$.

FIG. 15-a-b-c-d-e-f. Con¿dence region of the random acceleration dB (vertical axis) for DOF number j_{obs3} (inside point) over the MF band $[1600, 1900]$ Hz (horizontal axis) as a function of δ_M, δ_D and δ_K: deterministic response of the mean model (mid irregular thin solid line), mean value of the random response of the stochastic model (mid regular thin solid line), lower and upper envelopes of the con¿dence region corresponding to the probability level 0.95 (lower and upper thick solid lines).

FIG. 16-a. $\delta_M = 0, \delta_D = 0, \delta_K = 0.02$.

FIG. 16-b. $\delta_M = 0, \delta_D = 0, \delta_K = 0.3$.

FIG. 16-c. $\delta_M = 0, \delta_D = 0, \delta_K = 0.5$.

FIG. 16-d. $\delta_M = 0, \delta_D = 0.3, \delta_K = 0$.

FIG. 16-e. $\delta_M = 0, \delta_D = 0.5, \delta_K = 0$.

FIG. 16-a-b-c-d-e. Graph of the probability density function $e \mapsto p_{\mathcal{E}_n}(e)$ for the stochastic dynamical system over the MF band $[1600, 1900]$ Hz as a function of δ_M, δ_D and δ_K.

FIG. 17-a. DOF number j_{obs1} (excitation point).

FIG. 17-b. DOF number j_{obs2} (free edge point).

FIG. 17-c. DOF number j_{obs3} (inside point).

FIG. 17-a-b-c. Con¿dence regions of the random acceleration dB (vertical axis) for DOF numbers j_{obs1} (excitation point), j_{obs2} (free edge point) and j_{obs3} (inside point) for overlapped bans B, B' and B'': (1) deterministic response of the mean model over broadband MB band $[1400\,, 2100]$ Hz (mid irregular thin solid line), (2) lower and upper envelopes of the con¿dence regions corresponding to the probability level 0.95: MF band B' (lower and upper thick dashdot lines), MF band B'' (lower and upper thick dashed lines), MF band B (lower and upper thick solid lines).

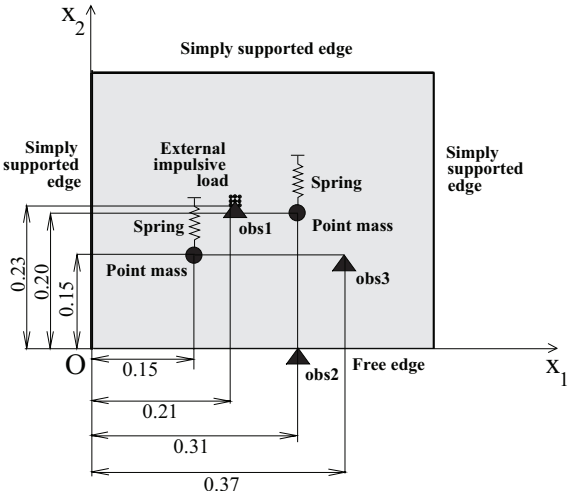

Fig. 1, C. Soize , J. of Eng. Mechanics

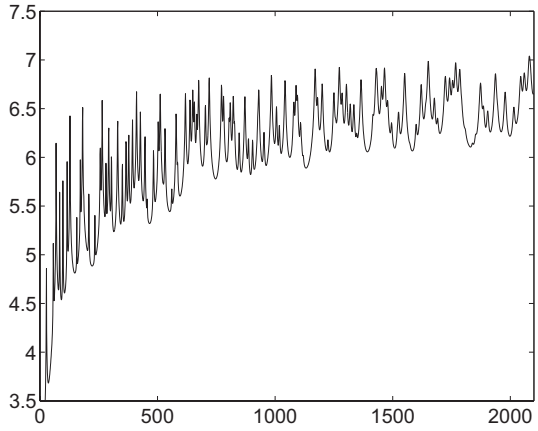

Fig. 2, C. Soize , J. of Eng. Mechanics

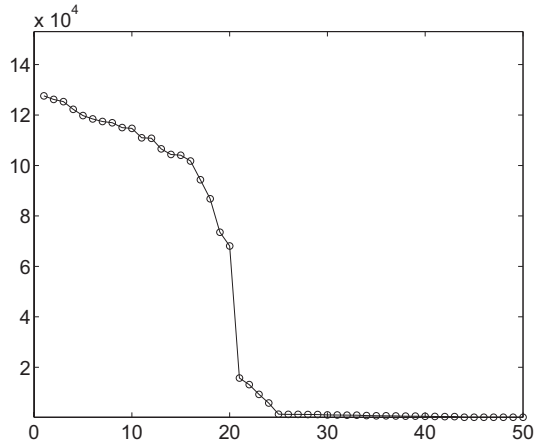

Fig. 3, C. Soize , J. of Eng. Mechanics

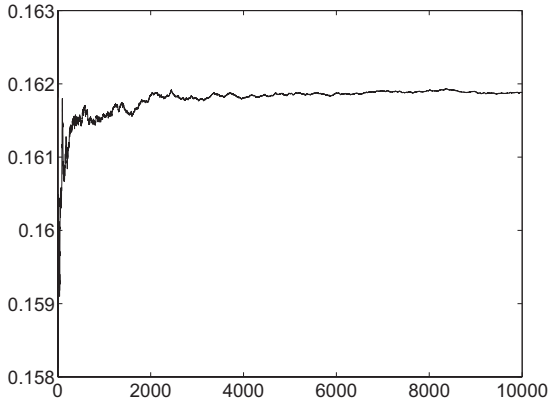

Fig. 4, C. Soize , J. of Eng. Mechanics

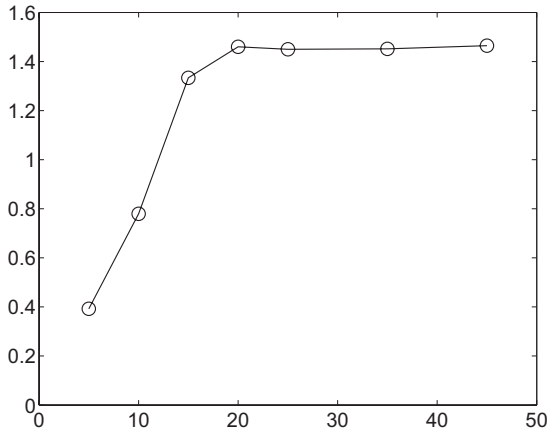

Fig. 5, C. Soize , J. of Eng. Mechanics

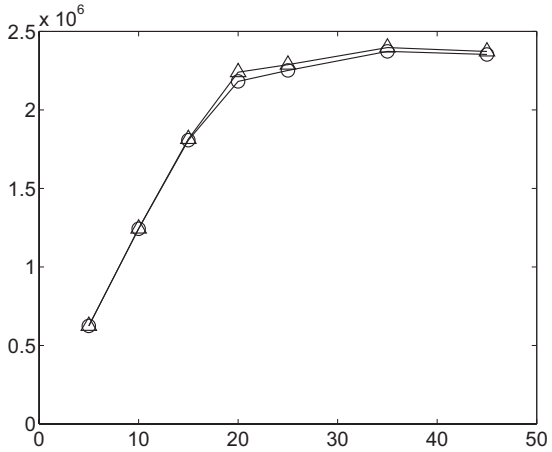

Fig. 6, C. Soize , J. of Eng. Mechanics

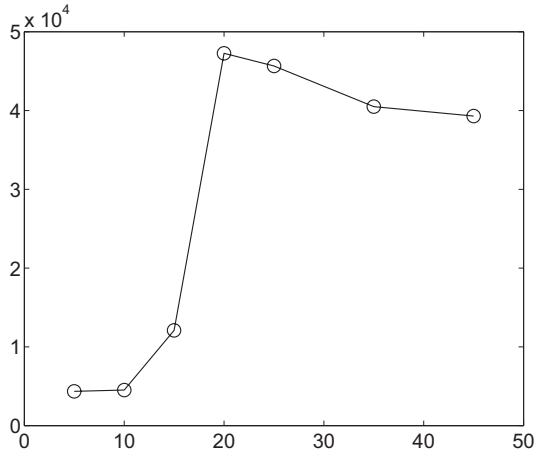

Fig. 7, C. Soize , J. of Eng. Mechanics

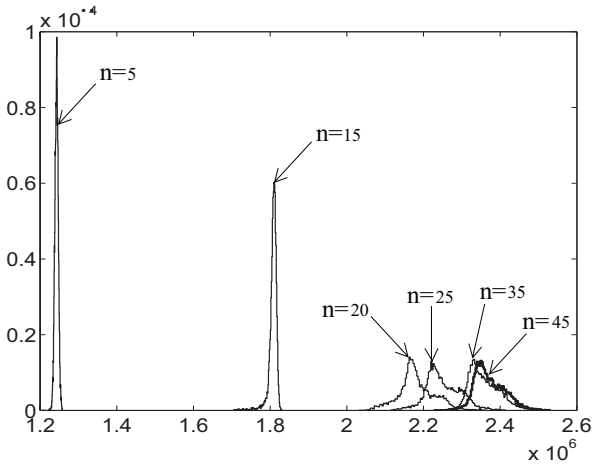

Fig. 8, C. Soize , J. of Eng. Mechanics

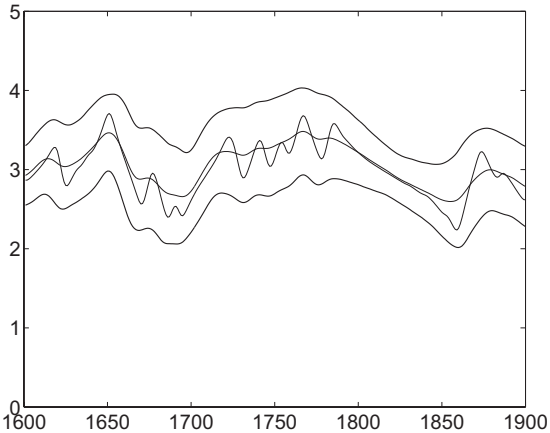

Fig. 9-a, C. Soize , J. of Eng. Mechanics

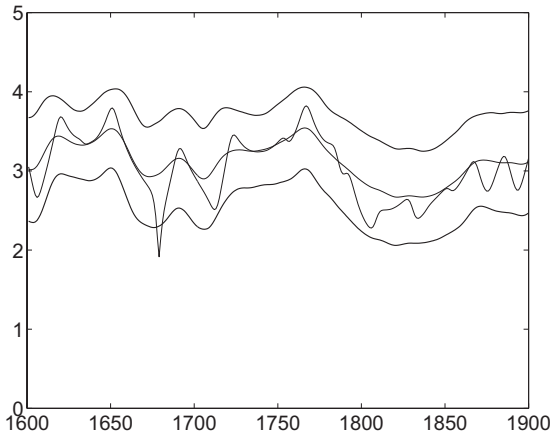

Fig. 9-b, C. Soize , J. of Eng. Mechanics

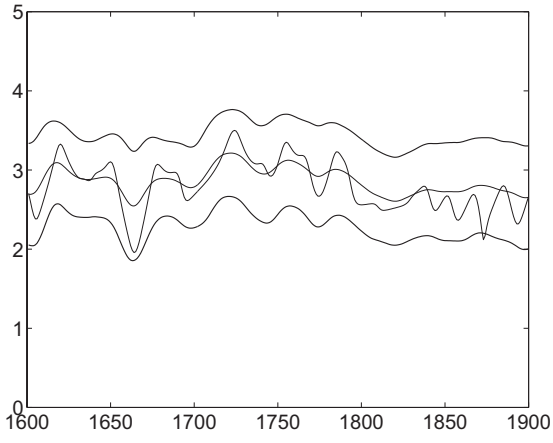

Fig. 9-c, C. Soize , J. of Eng. Mechanics

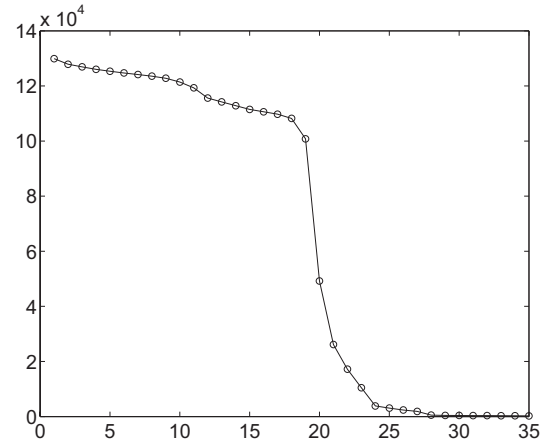

Fig. 10, C. Soize , J. of Eng. Mechanics

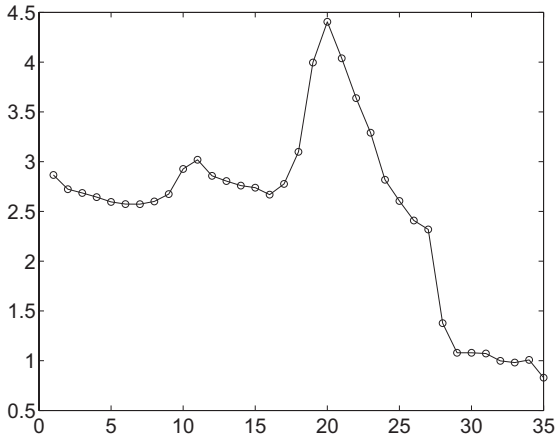

Fig. 11, C. Soize , J. of Eng. Mechanics

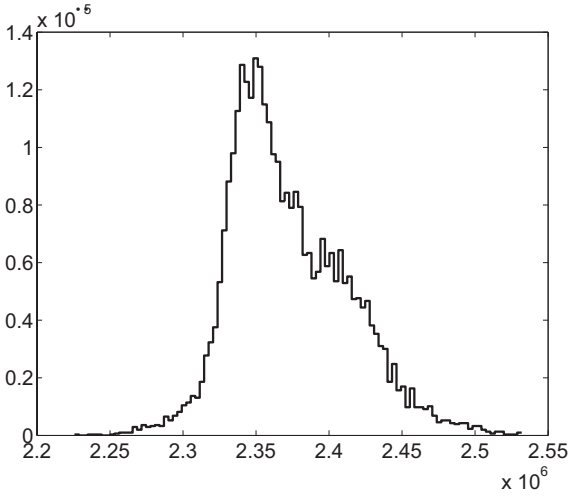

Fig. 12, C. Soize , J. of Eng. Mechanics

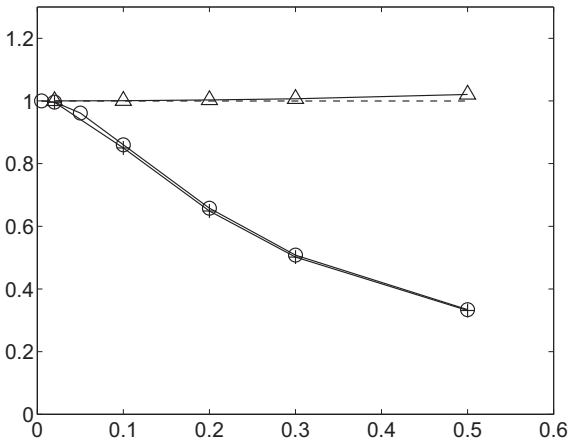

Fig. 13, C. Soize , J. of Eng. Mechanics

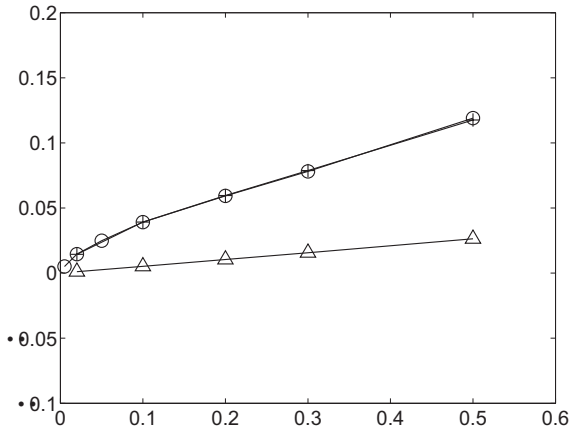

Fig. 14, C. Soize , J. of Eng. Mechanics

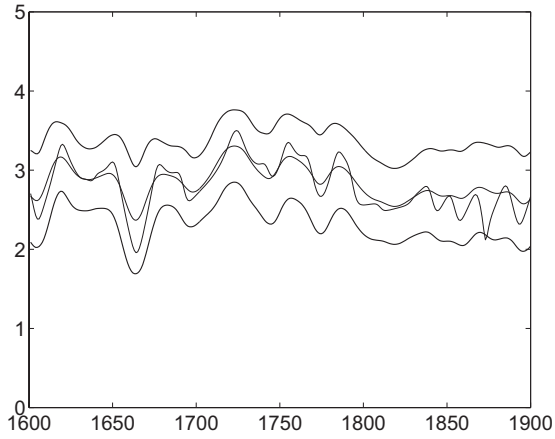

Fig. 15-a, C. Soize , J. of Eng. Mechanics

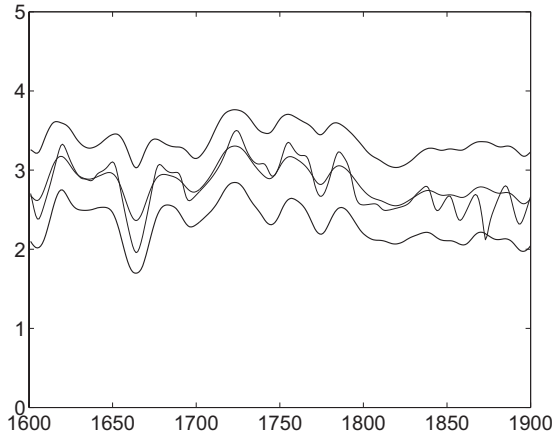

Fig. 15-b, C. Soize , J. of Eng. Mechanics

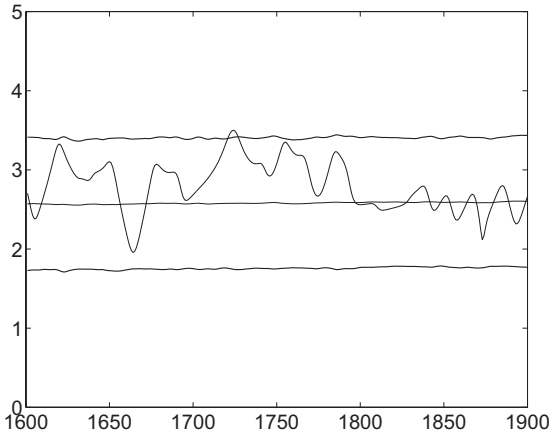

Fig. 15-c, C. Soize , J. of Eng. Mechanics

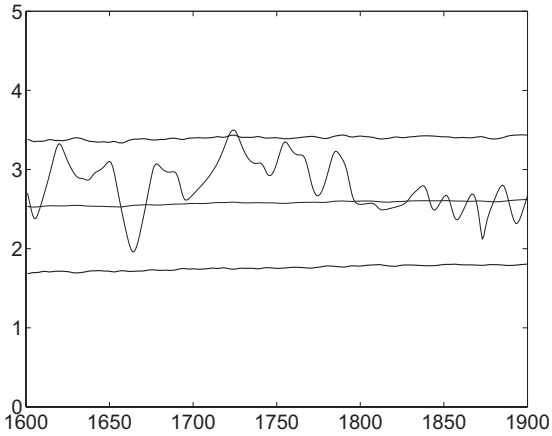

Fig. 15-d, C. Soize , J. of Eng. Mechanics

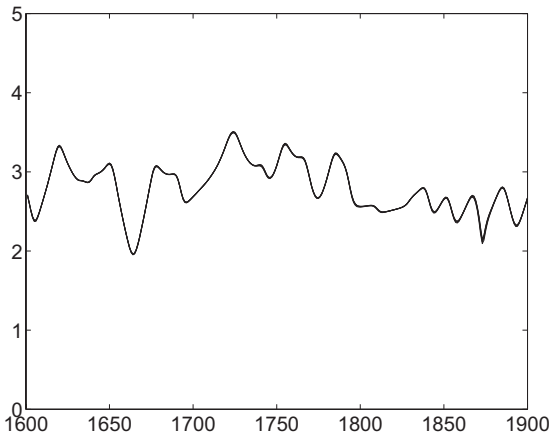

Fig. 15-e, C. Soize , J. of Eng. Mechanics

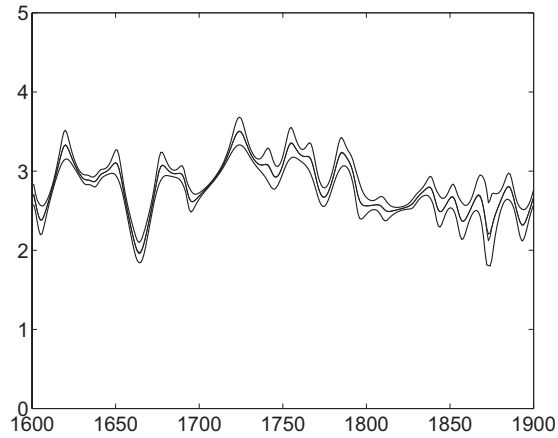

Fig. 15-f, C. Soize , J. of Eng. Mechanics

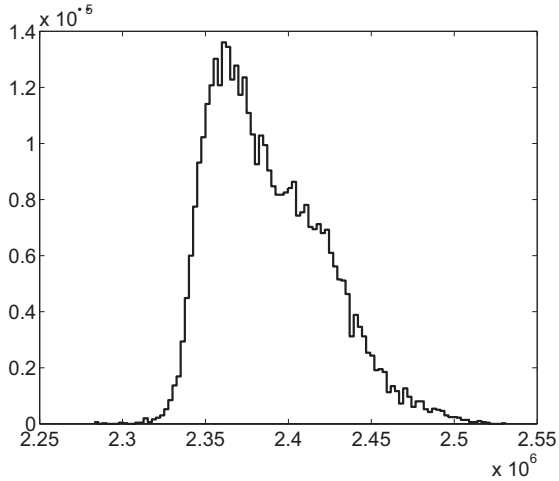

Fig. 16-a, C. Soize , J. of Eng. Mechanics

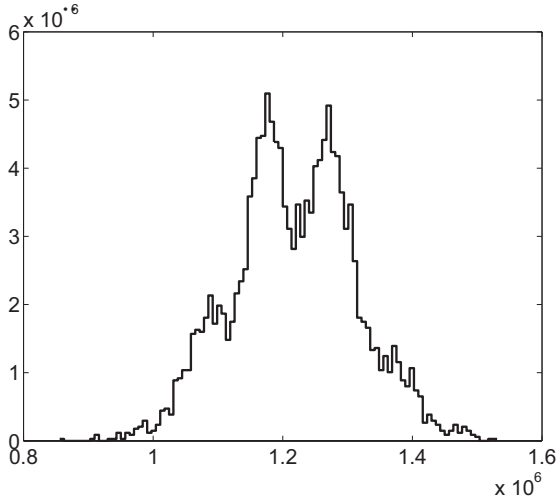

Fig. 16-b, C. Soize , J. of Eng. Mechanics

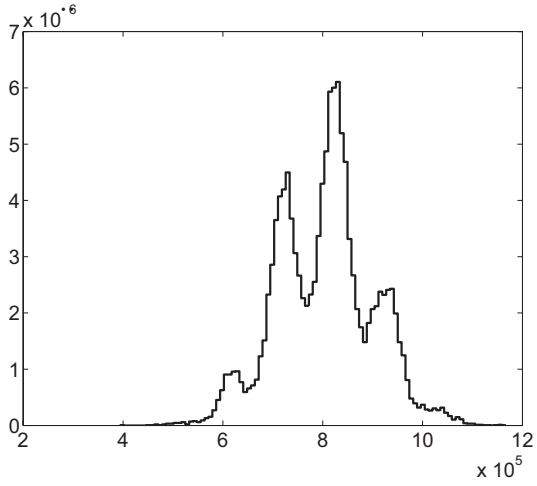

Fig. 16-c, C. Soize , J. of Eng. Mechanics

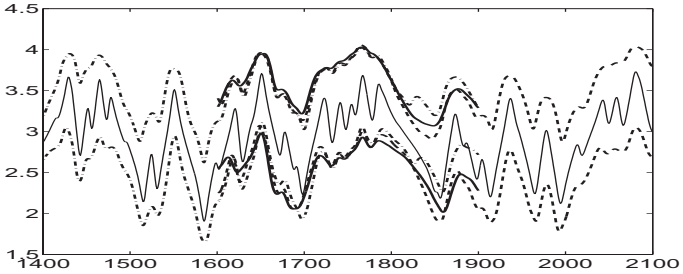

Fig. 17-a, C. Soize , J. of Eng. Mechanics

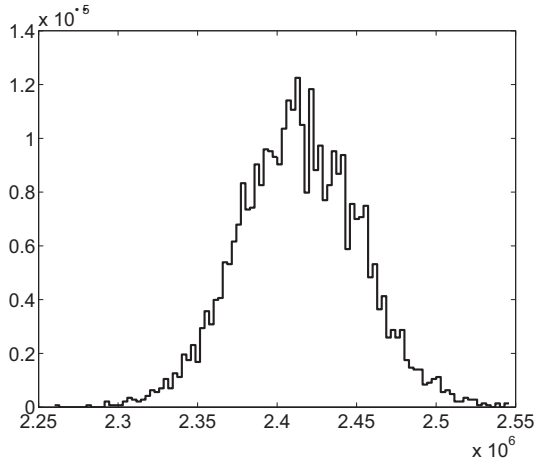

Fig. 16-d, C. Soize , J. of Eng. Mechanics

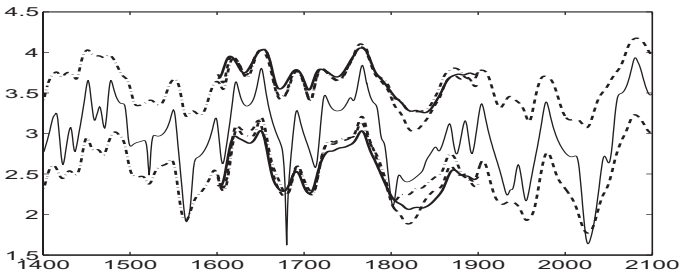

Fig. 17-b, C. Soize , J. of Eng. Mechanics

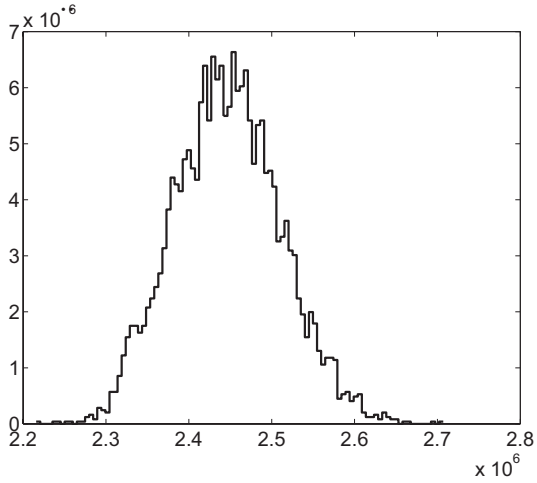

Fig. 16-e, C. Soize , J. of Eng. Mechanics

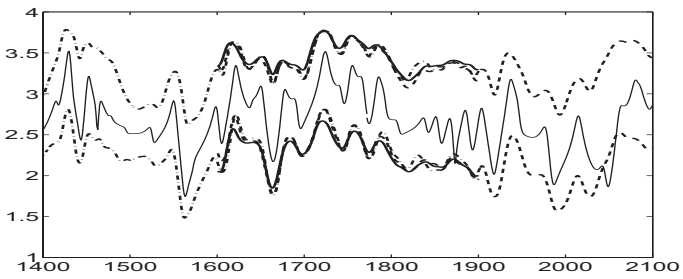

Fig. 17-c, C. Soize , J. of Eng. Mechanics